EARTH'S CRYOSPHERE
SCIENTIFIC JOURNAL

Kriosfera Zemli, 2020, vol. XXIV, No. 4, pp. 5–16 **http://www.izdatgeo.ru**

CRYOLITHOGENESIS

DOI: 10.21782/EC2541-9994-2020-4(5-16)

FEATURES OF FORMATION OF THE COMPOSITION OF RELIC GROUND VEINS IN THE BASE OF COVERING DEPOSITS IN THE FOREST-STEPPE OF THE TOBOL RIVER REGION

S.I. Larin[1], V.A. Alekseeva[2], S.A. Laukhin[3], N.S. Larina[4], V.L. Guselnikov[5]

[1]*Earth Cryosphere Institute, Tyumen Scientific Centre SB RAS, 86, Malygina str., Tyumen, 625026, Russia; silarin@yandex.ru*
[2]*Lomonosov Moscow State University, Faculty of Geography, 1, Leninskie Gory, Moscow, 119991, Russia*
[3]*Ordzhonikidze Russian State Geological Prospecting University, Faculty of Hydrogeology, 23, Miklukho-Maclay str., Moscow, 117997, Russia*
[4]*Tyumen State University, Institute of Chemistry, 6, Volodarskogo str., Tyumen, 625003, Russia*
[5]*LLC EcoStroiPererabotka, 1, Chernyshevskogo str., Tyumen, 625001, Russia*

The results of studying of the morphology and material composition of relic polygonal structures – small cracks, pockets, and larger wedge-shaped veins, stripped at the base of the covering carbonated deposit strata within the second fluvial terrace of the Tobol River valley – are presented. The particle size distribution analysis of the studied deposits displays the predominance of the coarse silt and fine sand fractions. The quartz grain surface textures reveal the predominance of sand grain with aeolian processing (up to 92 %). The total fraction of particles with eluvial features and traces of water transfer is small and ranges from 0 to 12–16 and 4 to 8 %, respectively. The particle roundness ratio varies from 51 to 59 %, averaging 54 % through the vein section. High values of the quartz grain fraction with traces of cryogenic processing (60–84 %), as well as the coefficient of cryogenic contrast (1.03–1.99) reflect the intense manifestation of cryogenic processes during the vein formation. Geochemical proxies and major element indices demonstrate a low degree of hypergenic transformation of the sediments filling the veins. The obtained data have revealed that the formation of the studied structures as originally ground veins in the active layer (possibly together with drying cracks), had occurred in the second half of the Sartan cryochron and at the beginning of the Holocene.

Cryogenesis, polygonal structures, covering deposits, Sartan cryochron, particle size distribution analysis, quartz grain surface texture, cryogenic contrast ratio, geochemical indices, aeolian processes

INTRODUCTION

In the south of Western Siberia and in Northern Kazakhstan, at the base of the covering deposits, many sections with relic vein structures are known. Extremely controversial opinions are expressed regarding their origin. In one case, they are considered to be cryogenic formations – pseudomorphs along ice wedges [*Fedorovich, 1962*], in another one, they are interpreted as cracks of arid drying, noting that the appearance of the network of cracks has nothing in common with the morphology of permafrost formations [*Volkov et al., 1969*]. As a result of the latest studies of these structures, their Sartan age has been revealed (MIS 2). At that time, in the southern part of Western Siberia, an arid extreme continental climate dominated, the periglacial landscapes of the cold tundra, tundra-steppes and forest-steppes were widely developed [*Zykin et al., 2001; Velichko, 2009*], low-temperature permafrost was formed (below –3 °C) with the active development of frost cracking and the formation of polygonal structures [*Fotiev, 2009*].

Within the Tobol–Ishim interfluve, thickness of permafrost reached 300–500 m, rock temperature dropped to –5 °C [*Baulin et al., 1981; Dynamics..., 2002; Fotiev, 2009; Velichko, 2009*]. The findings of pseudomorphs along with ice wedges at 52° N [*Zubakov, 1970; Arkhipov, 1971; Kaplyanskaya, Tarnogradsky, 1972*] and even at 50° N [*Zykin et al., 2001*] made it possible to draw the southern boundary of permafrost rocks in Sartan Ice Age in Western Siberia at 50–47° N [*Baulin et al., 1981*]. From the early Holocene (11,000 BP) to the end of the Holocene climatic optimum epoch, the stable and significant climate warming occurred in comparison with the Sartan age, the temperature of rocks was increased to positive values, and the active degradation of cryogenic strata of the Neopleistocene age took place [*Fotiev, 2009*].

The findings of relic vein structures in the forest-steppe and subtaiga of Trans-Urals give new information about the features of the permafrost zone in the southwest of Western Siberia in the Sartan cryochron epoch [*Laukhin et al., 2012; Larin et al., 2015, 2016, 2018*]. The paper presents the studying results of the morphology and material composition of vein structures stripped at the base of covering sediments

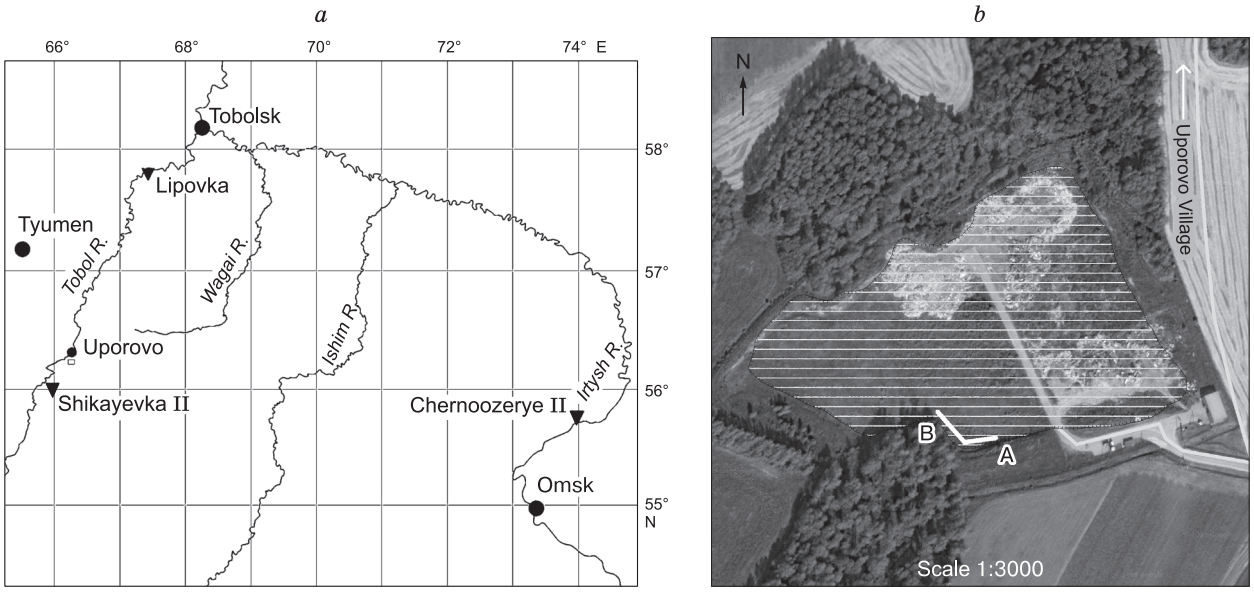

Fig. 1. Location of objects:

a – a section with relic polygonal structures in the sand pit nearby Uporovo Village of the Tyumen Oblast; Paleolithic sites of Shikayevka II, Chernoozerye II; the section of Lipovka; *b* – the location of the walls A and B in the sand pit nearby Uporovo Village.

which overlay the surface of the second right-bank twenty-meter-high terrace of the Tobol River [*Volkov et al., 1969*] near the terrace joint at an absolute elevation of 111 m. The section itself has been stripped in the walls of a sand pit which is currently used for landfill of municipal solid waste. The sand pit is located 4 km from the southern outskirts of Uporovo Village, Tyumen Oblast (56°16′01.91″ N, 66°17′00.75″ E), 109 km southeast of Tyumen City (Fig. 1). The height of the section above the water edge of Tobol River nearby Uporovo Village is 56.7 m.

GENERAL STRATIGRAPHY OF THE SECTION AND MORPHOLOGY OF VEINS

To study the stratigraphy and morphology of veins through the section, a south wall (wall A, length is 12.5 m; veins 1–9) and south-southwest one (wall B, length is 21.4 m; veins 10, 11, 11a, 12–15) of the sand pit have been stripped (Fig. 1, *b*). The generalized structure of the section from top to bottom is displayed in Fig. 2, 3.

1. Sod, humus horizon of current soils with traces of anthropogenic impact. Thickness is 0–70 cm. Vital signs of burrowers, plant roots up to a depth of 20–70 cm from the surface.

2. The fine, fine-grained and silty sand, tan and brown, dense, layered (on cutting planes), vertical fracturing is noticeable. Thickness of layer is from 25 to 112 cm, the average thickness is 81–82 cm. In the section near the veins 1 and 2, at the base of the horizon, into the depth interval of 57–80 cm, there is an interlayer of yellowish-brown, cross laminated coarse sand and gravel (up to 0.5 cm in size).

3. The fine-grained and silty sand, bluish-gray, horizontally laminated and lenticular layered, ferruginous in separate layers up to the thickness of 5 cm. On the general background, there are noticeable sparse oval bluish-gray spots (up to 1 cm in diameter) and vital signs of burrowers. Stripped up to a depth of 220–370 cm from the surface; below 190 cm the number of layers of coarser sand with a bluish and ocher color increases. The upper boundary of the layer is distinctly sharp, broken by a dense network of small, often wedge-shaped cracks and pockets up to 3–10 cm deep and 1–2 cm wide at the top, as well as larger veins 70–90 cm deep and up to 7–28 cm wide in the upper part. The cracks and veins are completely filled with material of overlying deposits of the second layer. The distances between the median axes of the upper part of the largest veins along the wall A are: 1/2 – 268 cm; 2/3 – 139 cm, 3/4 – 102 cm, 4/5 – 58 cm, 5/6 – 75 cm, 6/7 – 425 cm, 7/8 – 125 cm, 8/9 – 56 cm; those along the wall B are: 9/10 – 373 cm, 10/11 – 246 cm, 11/11a – 205 cm, 11a/12 – 276 cm, 12/13 – 305 cm, 13/14 – 735 cm. Most of the veins are wedge-like. Some of them are inclined, band-shaped, branching in the lower part, forming numerous apophyses in the form of thread-like tails or narrow cracks. The penetration depth of veins 1–9 (wall A) is 120–180 cm from the surface, the vertical length from the base of the second layer is 70–90 cm; those of veins 10–15 (wall B) are 150–203 cm and 50–120 cm, respectively.

Through all walls of the section, starting from a depth of 30–45 cm, but especially in the interval of from 80–110 to 120–165 cm, the carbonates are

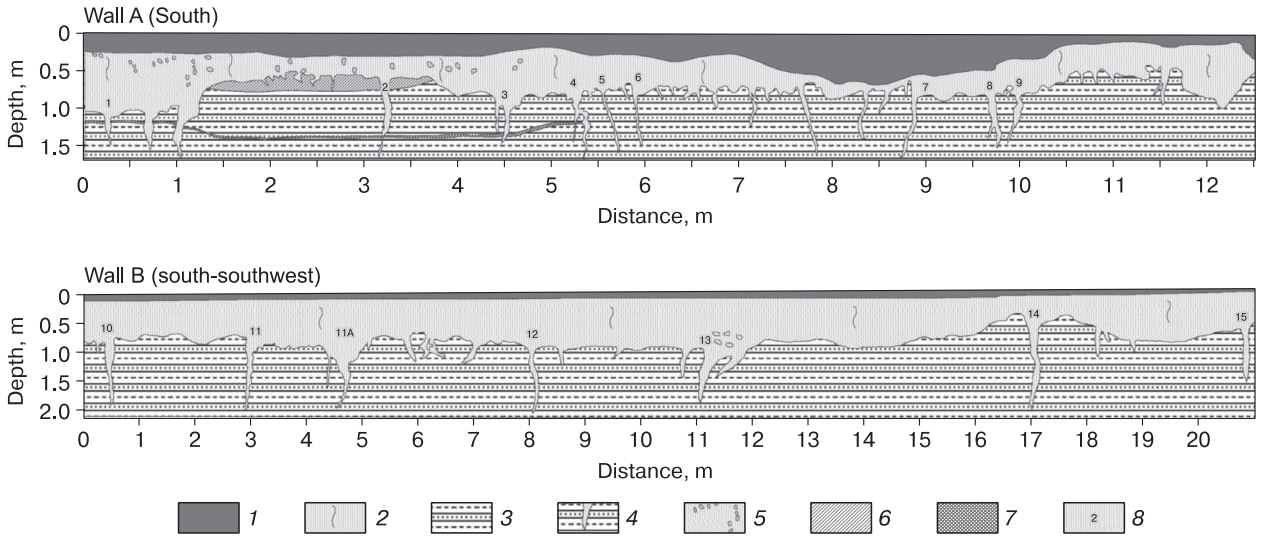

Fig. 2. Structure of upper part of section in walls of the sand pit nearby Uporovo Village of the Tyumen Oblast.

1 – soddy humus horizon of current soils; *2* – fine, fine-grained and silty sand, tawny and brown with vertical cracks; *3* – silty and fine-grained sand, bluish-gray, horizontally-laminated and lenticular-layered; *4* – ground veins; *5* – large carbonate nodules; *6* – a lens of cross-layered coarse sand with small pebbles; *7* – an interlayer of coarse sand of ocher color; *8* – numbers of veins.

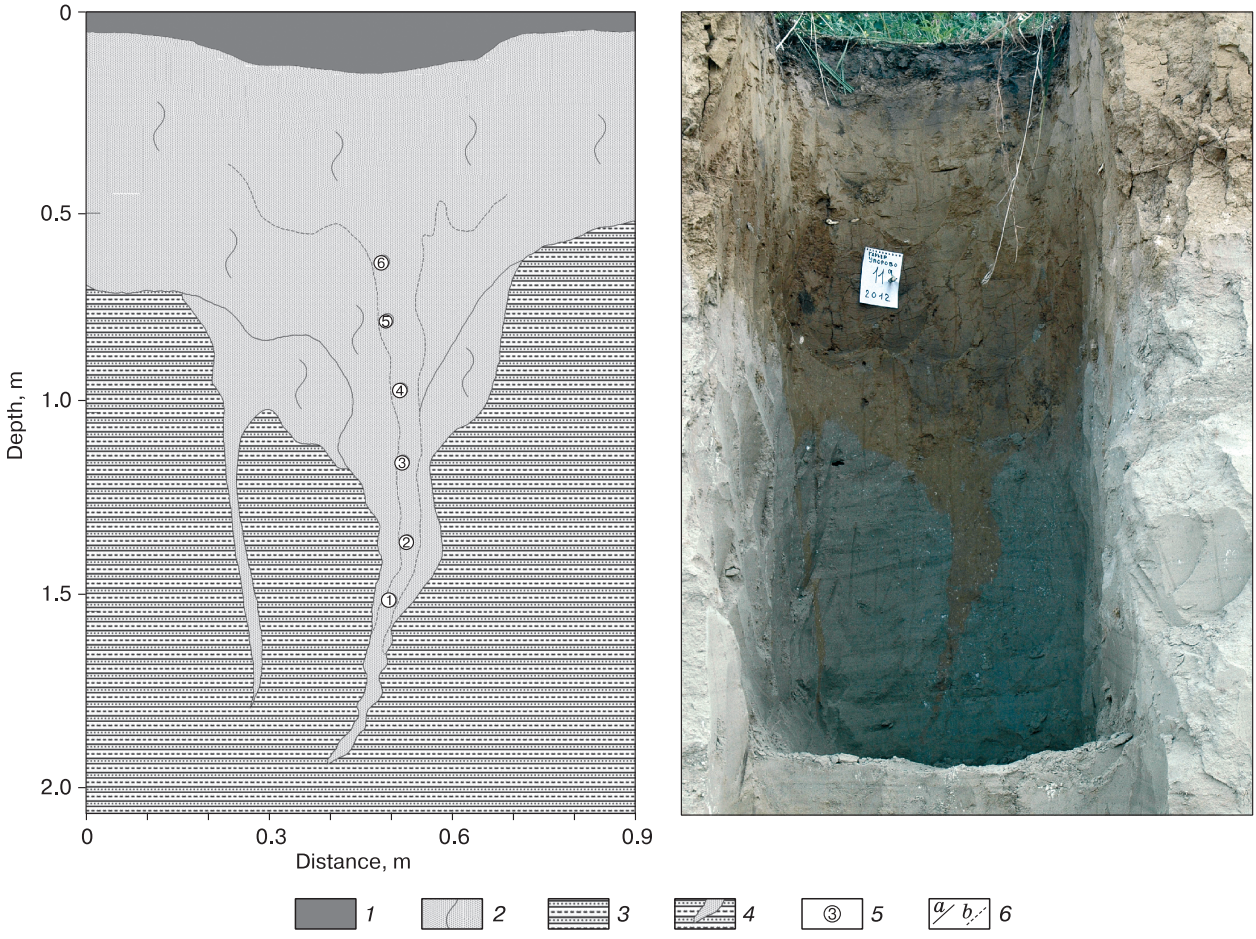

Fig. 3. Structure of vein 11a.

1–4 – see legend in Fig. 2; *5* – sampling sites and their numbers; *6* – boundaries: *a* – distinct, *b* – unclear.

abundant in the form of scattered whitish spots out of individual grains with a diameter of 0.2–0.3 mm, dense rounded nodules up to 1–2 in size cm, as well as stripes elongated from top to bottom. In some cases, carbonates literally "impregnate" and cement a very dense layer of enclosing sediments. The largest accumulations of carbonates have been noted in the wall A at a depth of 110–130 cm; two levels of carbonates have been fixed through wall B at the depths of 84 and 120–165 cm from the surface. In the central part of the vein 3, at a depth 70–90 cm, there are visible black vertical stripes in the form of gouges.

AGE OF POLYGONAL STRUCTURES

Information on the age of polygonal structures is provided by traces of frost cracking and cryogenic wedge-shaped disturbances, found in the walls of the excavations of the Paleolithic sites of: Shikayevka II in the Vargashinsky district of the Kurgan Oblast on the right bank of the Tobol River, and Chernoozerye II in the Sargat district of the Omsk Oblast on the left bank of the first fluvial terrace of the Irtysh River [*Zeitlin, 1979; Petrin, 1986; Gorbunova et al., 2016; Osintseva, 2017*]. The calendar dating below has been performed by F.E. Maximov (St. Petersburg State University) using the program OxCal 4.3 [*Reimer et al., 2013*].

The Shikayevka II site (Fig. 1, *a*) is located at a distance of 35 km south of the studied section on the western shore of Slobodchikovo Lake. The lake is located 10–12 km from the Tobol River. The water edge in the lake does not exceed 15 m above the floodplain. The age of sediments, containing cultural remains and mammoth fauna, underlying sediments with traces of paleocryogenesis, has been determined to be 13,000–11,000 BP [*Petrin, 1986*]. Judging by a rib of the mammal, torn by a relic wedge-shaped structure, traces of cryogenesis can be associated with increased cooling in MIS 1 (10,300–10,800 BP) [*Zeitlin, 1979*]. Later, radiocarbon dating of 18,050 ± 95 BP has been obtained by the mammoth bone from that site (21,870 ± 150 calendar years, SOAN-2211) [*Derevyanko et al., 2003*].

According to radiocarbon dating of charcoal, the age of the cultural horizons of the Chernoozerye II site (Fig. 1, *a*), deformed by later cryogenesis, is 14,500 ± 500 BP (17,610 ± 630 calendar years) (GIN-622) [*Zeitlin, 1985*]. A radiocarbon dating of 10,526 ± 44 BP has been obtained (12,490 ± 70 calendar years) (MAMS-27135) [*Gorbunova et al., 2016; Osintseva, 2017*] by a fragment of the bone, taken from the roof of the buried soil horizon at a depth of about 1.4 m.

Three horizons with initially wedge-shaped ground veins of small sizes (up to 0.5 m) have been identified [*Larin et al., 2015*] in the section of Lipovka (57°49′20.6″ N, 67°23′18.5″ E), located within the second fluvial right-bank terrace (20–25 m high) of Tobol River, 184 km downstream from the section nearby Uporovo Village (Fig. 1, *a*), above the layer with a dating of 21,400 ± 290 BP (25,690 ± 290 calendar years) (LU-7259), in the depth interval of from 0 to 12 m from the surface.

Thus, the radiocarbon dating of the Shikayevka II and Chernoozerye II Paleolithic sites, as well as the section of Lipovka, indicate the formation of cryogenic wedge-shaped structures at the base of the covering deposits of the territory under consideration in the Late Neopleistocene within the range of 25,600–12,400 BP.

Judging by a radiocarbon dating of 10,526 ± ± 44 BP (12,490 ± 70 calendar years), the youngest phase of cryogenesis took place during the severe and abrupt cooling in the Late Dryas (11,000–10,300 BP). It can be assumed that the veins of the characterized section have been formed exactly at that time. To study the material composition of the vein filling of the section, the vein 11a has been examined in detail.

DEPOSIT COMPOSITION: RESEARCH METHODS

The particle size distribution of the deposits of the vein 11 was studied by the sieve method using a standard set of sieves [*Voronin, 1986*]. A fraction of less than 0.01 mm was separated by elutriation from the pre-dispersed sample. To characterize the conditions of transportation and accumulation of sediments, the surface textural analysis of quartz grains was used. The sample preparation was carried out according to the previously tested technique [*Alekseeva, 2005*]. The samples were sprayed with gold as conductive material. The shape and surface texture of quartz grains were studied for the fraction of medium (0.25–0.5 mm) sand using the scanning electron microscope SEM TESCAN VEGA 3 LMU at an accelerating high voltage of 15–30 keV, in SE mode (Secondary Electron Image) and in high vacuum with magnification from 300–400 times (for whole grains) to 1,500–2,000 times (for grain fragments, individual surface elements). In each sample, 25 randomly selected quartz grains were studied. When describing the grain, three groups of attributes were evaluated: 1) general morphological features (the shape and manifestation of the grain surface relief); 2) surface textures formed as a result of mechanical action on grains (textures, steps, fracture plates, scratches, grooves, V-shaped pits, upturned plates, etc.); 3) structures having a chemical origin (traces of etching, accumulation of adhering particles, silica films, etc.). The roundness of quartz grains was evaluated visually, on a five-point scale. For each sample, the roundness ratio (characterizing the average roundness of grains in a sample) was calculated using the

formula proposed by A.V. Khabakov [*1946*]. The combination of the quartz sand grain surface textures, based on the ideas of various researchers [*Mahaney, 2002; Alekseeva, 2003, 2005; Krinsley, Doornkamp, 2011; Vos et al., 2014*], was used to reveal their origin.

The cryogenic contrast ratio (*CCR*) has been calculated as a quantitative indicator of the degree of participation of cryogenesis in the filling of vein structures. That permafrost-climatic indicator, independent of petrographic composition and terrigenous-mineralogical provinces, takes into account the distribution of quartz and feldspars according to the particle size spectrum [*Konishchev, Rogov, 1994*].

$$CCR = (Q_1/F_1) / (Q_2/F_2),$$

where Q_1/F_1 is the ratio of the content of quartz to that of feldspars in the fraction of 0.05–0.01 mm; Q_2/F_2 is the same ratio in the fraction of 0.1–0.05 mm.

The values of *CCR* more than 1 demonstrate the decisive role of cryogenic factors in the complex of hypergenic processes, depending on which the particle size distribution of sediment is formed. The values of *CCR* less than 1 indicate the formation of deposits in a relatively warm climate with a subordinate role of cryogenic processes. The content of quartz and feldspars in the sediment fractions of 0.05–0.01 mm and 0.1–0.05 mm has been determined by X-ray diffractometry using a Bruker D2 Phaser diffractometer (CuK_α radiation, X-ray tube generator parameters: 30 kV, 10 mA). X-ray diagnostics of minerals has been carried out using a semi-quantitative comparison in powder databases ICDD PDF2 and COD phase analysis has been performed using the DIFFRAC.EVA package.

For an independent assessment of the palaeoclimatic conditions for the accumulation of sediments filling the vein structures, a geochemical approach has been used. It is based on the empirical dependences of the weathering coefficients coupling the changes in the gross chemical composition of deposits with climatic factors [*Alekseev et al., 2019*].

The chemical composition of the samples has been studied by a method of the X-ray fluorescence analysis (Spectroscan MAKC-GV X-ray spectrometer) according to the method for measuring the mass fraction of metals and metal oxides in powder samples. The average sample was ground to powder and placed in a special cuvette. The standard weight was at least 200 mg. Quantitative calibrations have been carried out using a set of state standard samples of the rock and soil chemical composition, as well as standard samples of rocks and soil obtained from the Institute of Geology of the University of Mexico City (Mexico) [*Lozano, Bernal, 2005*]. Based on the values of the chemical element's content in the samples of the deposits filling the vein 11a, the geochemical coefficients have been calculated. The geochemical coefficients are the indicators of sedimentation conditions [*Lukashev, 1970; Retallac, 2001, 2003*]: the silicate one ($K_i = SiO_2/Al_2O_3$) – the ratio of quartz (resistant to chemical weathering of the mineral) to feldspars (unstable components); the basiconic ($BA = (CaO + K_2O + Na_2O)/Al_2O_3$) – the ratio of mobile elements to inert aluminum (clay component); one of the chemical maturity ($K_z = Al_2O_3/Na_2O$) – the ratio of aluminum to maximum mobile sodium; the carbonate one ($K_k = CaO/MgO$) – the ratio of calcium to magnesium – the ratio of calcium and magnesium, reflecting the accumulation of calcite and dolomite; the alkaline one ($K_h = K_2O/Na_2O$) – the ratio of potassium to sodium, characterizing the behavior of readily soluble salts through the profile; the bioproductivity $(Fe_2O_3 + MnO)/Al_2O_3$; MnO/Al_2O_3; MnO/Fe_2O_3 $(Fe_2O_3 + MnO)/Fe_2O_3$ [*Vlag et al., 2004; Kalinin et al., 2009*]; degree of homogeneity of TiO_2/Al_2O_3 and Zr/TiO_2 rocks [*Schilman et al., 2001*]; the resistance of various minerals to weathering (Rb/Sr), namely mica and potassium feldspars, with which rubidium is associated, and carbonates, with which strontium is associated [*Gallet et al., 1996*]; Sr/Ba – reflects the hydrothermal conditions of sediment accumulation [*Syso, 2007*], in particular, the leaching process, while strontium is associated with carbonates [*Perelman, 1989*], and barium is associated with potassium feldspar and is harder removed out of soils and sediments. In the interfluve rock of Western Siberia, the Sr/Ba ratios increase as the climate aridity increases from north to south, from 0.2 or less in the over-moistened northern taiga of the Pur Lowland to 1.4 in the dry steppes of the Kulunda Plain [*Syso, 2007*].

The degree of maturity of a substance is coupled with the climatic conditions. The most profound transformations of the material composition of sediments occur in warm and hot humid climates, and minimal ones take place in cold arid climate [*Perelman, 1989*]. The larger the values of K_i, K_z, and the less those of *BA*, the higher the degree of chemical maturity of the material.

A detailed analysis of the use of the proposed indicators and a number of the others, as well as the rationale for that approach, has been presented in a number of publications in recent years [*Kalinin et al., 2009; Sheldon, Tabor, 2009; Kalinin, Alekseev, 2013; Alekseeva et al., 2016; Alekseev et al., 2019*]. To identify cryogenic conditions, the geochemical indexes *CIA*, *CIW*, and *ICV* have been calculated. The weathering index $CIA = [Al_2O_3/(Al_2O_3 + CaO + Na_2O + K_2O)]\cdot 100$ reflects the ratio of primary to secondary minerals in the gross sample; it is used to obtain information on the weathering intensity and climatic conditions of sediment formation. In the cold arid climatic conditions, the slightly transformed unweathered rocks are characterized by lower values of *CIA* ~ 50, whereas for intensely-weathered rocks, formed in a warm humid climate, *CIA* is less than 100.

The threshold value for deposits formed in a cold arid climate is *CIA* ~ 70 [*Nesbitt, Young, 1982*]. A variation of *CIA* is *CIW* – the index of chemical conversion of deposits neglecting the effect of the biological cycle of potassium: $CIW = [Al_2O_3/(Al_2O_3 + CaO + Na_2O)] \times 100$ [*Fedo et al., 1995*]. The *ICV* index = $[Fe_2O_3 + K_2O + Na_2O + CaO + MgO + TiO_2]/Al_2O_3$ [*Cox et al., 1995*] reflects the degree of chemical maturity of thin aluminosilicoclastics entering the sedimentation area. The index of immature deposits with a high content of non-clay minerals is more than 1, that of more mature deposits with a large amount of clay minerals is less than 1.

RESULTS AND DISCUSSION

The analysis of the particle size distribution. In the granulometric composition of the material which fills the vein 11a, the sand fraction prevails with the content of the silt and clay particles within the range of 16–18 % (up to 28 % in the uppermost sample) (Fig. 4). From top to bottom, there is a change in the ratio of the dominant fractions of fine-grained and fine sand. The upper part of the vein is composed of fine-grained silty sand (according to the nomenclature of V.T. Frolov [*1993*]). Below the section, fine and fine-grained silty sand are exposed with a gradual decrease in the content of the fine sand fraction (from 41.2 to 34.85 %). The lowest sample can be classified as fine-grained and fine sand with a fine-grained sand fraction of 26.86 %.

The cryogenic contrast ratio. In the lower part of the vein section, the values of *CCR* (1.03–1.99) indicate a noticeable effect of cryogenesis on the filling deposits (Fig. 5). In the middle of the vein section, the effect of cryogenesis significantly either decreases or completely disappears (*CCR* = 0.14–0.75). In the upper part of the section, the role of cryogenic influence on vein's filling increases again (*CCR* = 1.35). The *CCR* values are genetically related to the mean annual temperature of the rock surface [*Konishchev, 1999; Konishchev et al., 2005*], therefore the *CCR* values of 1.03 corresponds to the conditions of the northern taiga with island permafrost and deep seasonal freezing.

The reconstructed mean annual temperatures of the rock surface are within the range of 0...–2 °C. The *CCR* values of 1.99 are the indicator of the sharp cooling and the decrease in the mean annual temperature of deposits up to –10...–11 °C. On the relationship graph of the *CCR* values and the mean annual rock surface temperature, that corresponds to the tundra-gley soils of the Arctic [*Konishchev, 1999; Konishchev et al., 2005*]. The *CCR* values of 0.75–0.14 indicate the positive mean values of rock temperature and the consistent decrease of the seasonal freezing depth. If the *CCR* is 0.75, relatively deep seasonal freezing is being reconstructed, if the *CCR* is 0.29 and 0.14, the depth of seasonal freezing is 0.7–0.8 m [*Konishchev, Rogov, 2016*]. The *CCR* value of 1.35 indicates the return of the existence conditions of island permafrost, deep seasonal freezing and a decrease in the mean annual soil temperature up to 0...–2 °C.

The quartz grain surface textures. The study of the sand particle fraction of 0.25–0.5 mm has demonstrated a predominance of semi-rounded grains of the II roundness class in the vein section (the frequency of occurrence along the section is from 48–60 to 76 %).The percentage of rounded grains (III–IV class of roundness) is 24–40 %, and that of angular ones (0–I class of roundness) varies from the first percents to 20 %. Correspondingly, the roundness ratio (according to A.V. Khabakov [*1946*]) is rather high (51–59 %), averaging 54 % in the section.

In the studied samples from the vein section, the quartz grains of three main types are found which bear signs of transportation and accumulation in various environments.

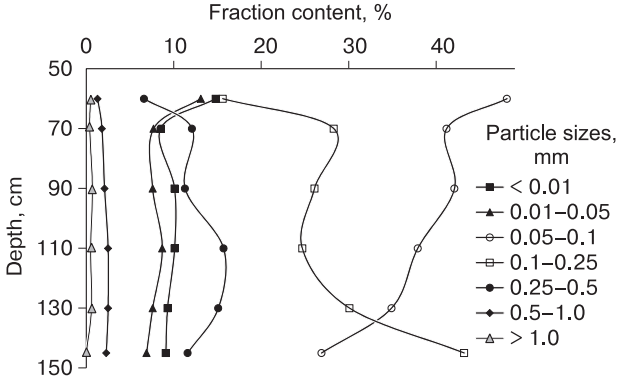

Fig. 4. Results of the particle-size distribution analysis of sediments filling vein 11a.

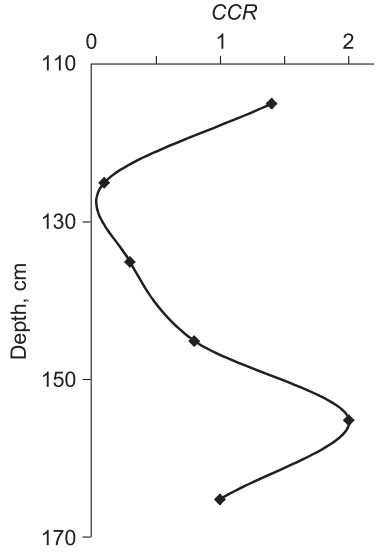

Fig. 5. Cryogenic contrast ratio (*CCR*) for samples out of vein 11a.

The first type includes angular particles of the I (less often of the II) roundness class, with sharp or slightly rounded edges and corners, with medium and high relief and surface, which is a combination of conchoidal fractures of various sizes, arcuate and straight steps and fractures plates. Such an appearance is characteristic of terrigenous eluvial grains which have not undergone a significant transfer in the aquatic environment (Fig. 6, *a*).

The second type of grains is represented by rounded particles (mainly of the III roundness class) with convex faces, with a low or medium relief; the surface of the particles is complicated by upturned plate sand straight scratches; conchoidal fractures,

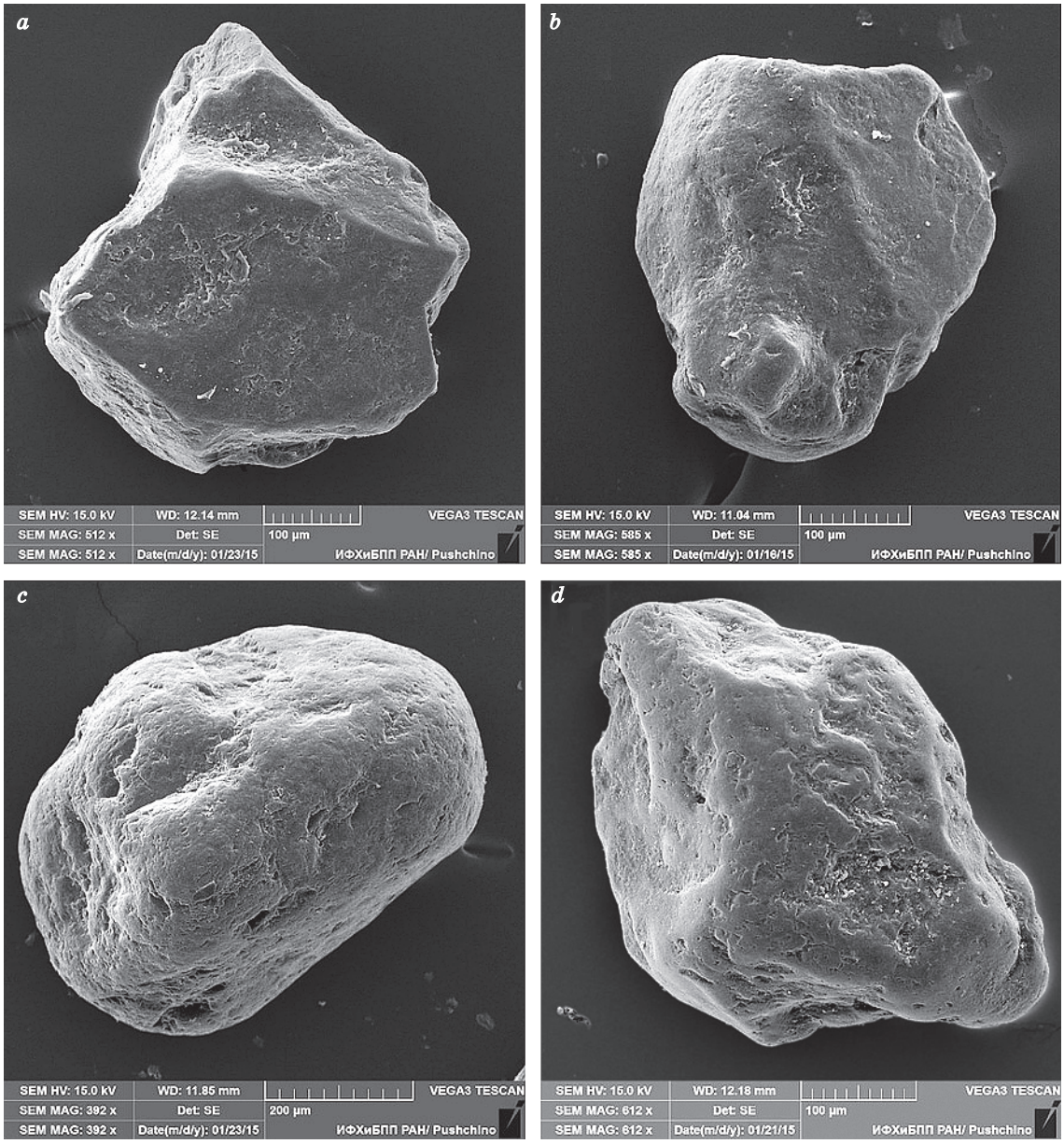

Fig. 6. Quartz grain surface texture of the 0.25–0.5 mm fraction out of the deposits of vein 11a:

a – quartz grain of eluvial group: angular shape, I roundness class, medium relief, sharp ribs and conchoidal fractures; surface is complicated by silica a film; *b* – quartz grain of eluvial group with features of aeolian transfer: semi-angular shape, II roundness class, medium relief and single conchoidal fractures, edges are smoothed with traces of edge abrasion, surface is complicated by upturned plates; *c* – quartz grain transformed during aeolian transfer: rounded shape with convex faces, III roundness class, medium relief, surface is complicated by upturned plates and curved grooves; *d* – quartz grain of eluvial group with features of water transfer: semi-angular shape, II roundness class, medium relief, there are V-shaped pits and curbed grooves aggravated by dissolution processes on unweathered surface, single accumulations of amorphous silica are observed in depressions.

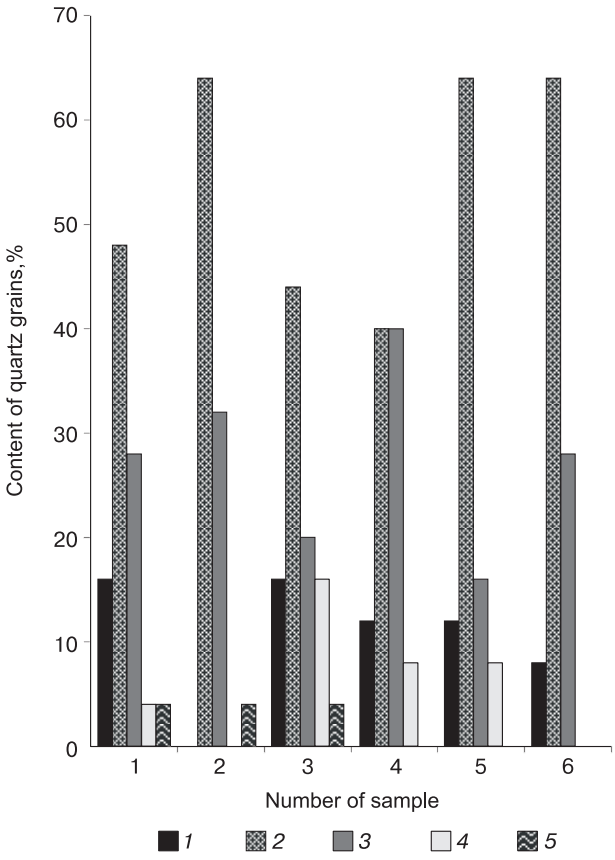

Fig. 7. Ratio of quartz grains of various morphogenetic groups in samples of vein 11a.

Morphogenetic groups: *1* – eluvial ones; *2* – ones with features of eolian transfer; *3* – ones with features of water transfer; *4* – eluvial ones with features of aeolian transport; *5* – eluvial ones with features of water transfer.

arcuate and straight steps are also found. Such a complex of elements is characteristic of the aeolian sedimentation environment, where the main factor in the formation of the surface of sand grains is the mechanical corrasion (Fig. 6, *c*). The intermediate type (between those two) can be classified as particles of semi-rounded form of the II (sometimes of the I or the III) roundness class, the surface of which bears traces of the combined effects of weathering and aeolian transportation (Fig. 6, *b*). The degree of manifestation of the aeolian processing features varies from the roundness of the corners and edges, and the convexity of the faces to a significant fraction (30 %) of upturned plates on the surface of sand particles.

The third type includes quartz grains of the II–III roundness class, with a low and medium relief, with often a smooth surface on which small conchoidal fractures, V-shaped pits with varying frequency of occurrence, straight scratches and cueved grooves are found. A significant degree of roundness, as well as a specific combination of surface textures, indicates processing in the aquatic environment (Fig. 6, *d*).

Thus, the main part of the sample is the particles which have undergone varying degrees of aeolian transportation: 40–64 % of medium-rounded aeolian grains with eluvial features, and 16–40 % of well-rounded aeolian grains (Fig. 7). On average, 81 % of particles have been transformed to a greater or lesser extent during the aeolian transportation. The content of the angular particles, which virtually have no traces of movement, ranges from 0 to 12–16 %, averaging 11 %. The total fraction of particles with traces of water transport on average does not exceed 4–8 %; only for sample 5 it is 20 %.

The results of the study have revealed a significant effect of cryogenic processes on vein's deposits in the form of various surface defects of quartz particles: chips, cracks and grooves. The proportion of the grains with surfaces of cryogenic origin in the section of the studied vein 11a varies from 60 to 84 %, averaging 69 % through the section. In addition to traces of crushing and splitting of sand quartz particles during cryogenic exposure, the formation of fine fractions during cyclic freezing-thawing is also observed. As a result, the films of deposited colloids are formed on quartz grains, under which particle destruction (cracking and fragment breaking-off) is observed [*Rogov, 2009*]. The surface of the vast majority of quartz grains in the samples is more or less complicated by silica deposition elements both in the form of silica films and in the form of concentrations of different thicknesses on flat surfaces, on the walls and bottoms of chips.

Geochemical proxies and major element indices. The gross chemical composition of the vein filling is characterized by relatively slight (within the limits of the method error) variability of the contents of SiO_2, Al_2O_3, Fe_2O_3, CaO, MgO, K_2O, Na_2O through the section profile (Fig. 8, *A*). Silica noticeably predominates (average values of the silicic ratio K_i is 5.6, the range of values is 4.8–5.9). The ratios of K_i, BA, K_z, K_k, K_h are characteristic of the harsh conditions of the northern geographical zones (Fig. 8, *B*). They are the indicators of the very low degree of weathering and chemical maturity of the vein-filling

Fig. 8. Values of geochemical proxies and major element weathering indices through the section of vein 11a.

A – oxide content (%): *1* – Na_2O, *2* – MgO, *3* – K_2O, *4* – Fe_2O_3, *5* – CaO, *6* – Al_2O_3, *7* – SiO_2; *B* – geochemical ratios: *1* – $BA = (CaO + K_2O + Na_2O)/Al_2O_3$, *2* – $K_h = K_2O/Na_2O$, *3* – $K_k = CaO/MgO$, *4* – $K_i = SiO_2/Al_2O_3$, *5* – $K_z = Al_2O_3/Na_2O$; *C* – ratios of bioactivity and bioproductivity level: *1* – MnO/Al_2O_3, *2* – MnO/Fe_2O_3, *3* – $(Fe_2O_3 + MnO)/Al_2O_3$; *4* – $(MnO + Fe_2O_3)/Fe_2O_3$; *D* – climate indices: *1* – *ICV*, *2* – *CIA*, *3* – *CIW*; *E* – degrees of geochemical homogeneity of rocks (*1*, *2*); mineral resistance to weathering (*3*); hydrothermal conditions for sediment accumulation (*4*).

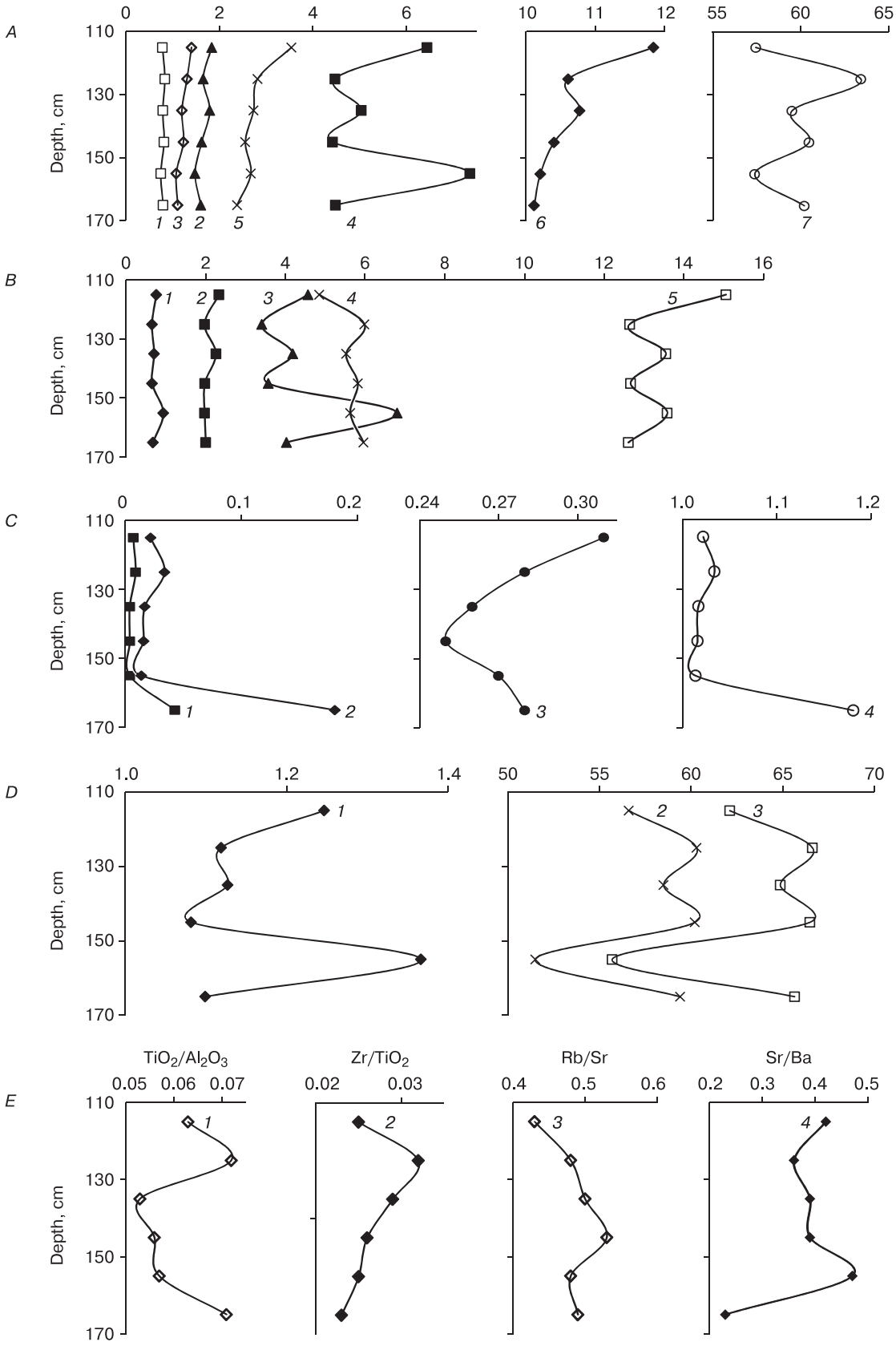
A
B
C
D
E
Depth, cm
110
130
150
170
0 2 4 6
10 11 12
55 60 65
1 3 2 5 4 6 7
0 2 4 6 8 10 12 14 16
1 2 3 4 5
0 0.1 0.2
0.24 0.27 0.30
1.0 1.1 1.2
1 2 3 4
1.0 1.2 1.4
50 55 60 65 70
1 2 3
TiO2/Al2O3
Zr/TiO2
Rb/Sr
Sr/Ba
0.05 0.06 0.07
0.02 0.03
0.4 0.5 0.6
0.2 0.3 0.4 0.5
1 2 3 4

deposits. The average values and range of values of the ratios: the basic one BA = 0.74 (0.66–0.94), the maturity one K_z = 13.35 (12.61–15.05), the alkaline one K_h = 2.0 (1.98–2.34), the carbonate one K_k = 4.43 (3.41–6.80).

The minimum values of the bioactivity and bioproductivity level ratios also reflect adverse climatic conditions during the vein filling (Fig. 8, *C*). That is especially noticeable in the lower part of the section of the vein 11a. The indexes (*CIA* = 51–60, *CIW* = 55–66, and *ICV* = 1.09–1.37 (Fig. 8, *D*)) are witnessed about the chemical immaturity of the vein-filling deposits, the high content of non-clay minerals and their formation under cryo-arid climatic conditions. The coldest climatic conditions are being reconstructed for the lower part of the vein fillings: *CIA* = 51, *CIW* = 55, *ICV* = 1.09.

The value distribution of the TiO_2/Al_2O_3 and Zr/TiO_2 ratios through the vein profile indicates a fairly homogeneous substrate formed on a parent rock (Fig. 8, *E*).

The relative softening of permafrost conditions, recorded by low values of cryogenic contrast ratio, correlates with a maximum weathering coefficient (Rb/Sr = 0.53) in the middle part of the vein section. Above the vein section, the Rb/Sr values decrease to 0.43, reflecting the deterioration of climatic conditions and the increasing of cryogenesis.

The values of the Sr/Ba ratio through the veins 11a lie within the range of 0.23–0.47 and correspond to the landscape-climatic conditions which are characteristic of the northern, and then higher in the section, southern and middle taiga [*Syso, 2007*]. It should be noted that the Sr/Ba ratio values correlate with the cryogenic contrast ratio and the distribution of carbonates and readily-soluble salts along the section.

CONCLUSIONS

1. The base of the carbonated covering sediments, overlaying the surface of the second right-bank terrace of Tobol River, is broken by wedge-shaped cracks, pockets and larger veins filled with the fine, fine-grained and silty sand of predominantly aeolian origin. About 92–96 % (an average of 81 % through the section) of quartz grains, to one degree or another, has experienced wind transfer. The average particle content of the eluvial and fluvial origin through the vein section is 11 and 4–8 %. The roundness ratio of the particle sample (according to A.V. Khabakov) on average through the section is 54 %.

2. Cryogenic processes have had a significant effect on the vein-filling deposits, manifested in the form of various surface defects of quartz particles: chips, cracks and grooves. The proportion of quartz grains with surfaces of cryogenic origin in the section of the studied vein 11a is 60–84 %. The values of cryogenic contrast ratio in the upper part of the vein section indicate the existence of the northern taiga landscapes with the mean annual rock surface temperatures in the range 0...–2 °C, with the development of island permafrost and deep seasonal freezing. In the lower part of the vein section, a short-term stage of severe permafrost and climatic conditions typical of the Arctic, with mean annual rock temperatures of –10...–11 °C has been recorded. In the middle part of the vein section, the *CCR* values indicate the positive average temperatures of the deposits and a noticeable decrease in the depth of seasonal freezing.

3. Geochemical data suggest on the poor transformability and chemical immaturity of the vein-filling deposits, their formation on a homogeneous parent rock, the noticeable influence of cryogenic factors on the filling of the veins and their formation in the range climatic conditions of the northern, middle and southern taiga.

4. Small vertical extent, the absence of downward folding structures of host-rock layers has allowed suggesting that the studied vein structures had been formed as initial soil, possibly together with drying cracks, which had arise as a result of frost cracking within the active layer. Judging by the low values of the reconstructed mean annual temperature of the deposits (up to –10...–11 °C at the base of the vein 11a), it is possible that in the initial stage they could develop like pseudomorphs over ice wedges in the relatively harsh conditions of the Late Dryas, although there is no other traces of that. Taking into account the data on the *CCR* and geochemistry, it can be assumed that the formation of initially ground veins proceeded under milder conditions of deep seasonal freezing or island permafrost in the beginning of the Holocene [*Romanovsky, 1977*]. During the evolution of polygonal structures, they have been filled mainly with aeolian material of overlaying sediments.

On the whole, such a palaeogeographic situation took place on the West Siberian Plain in the Sartan and late glacial periods [*Velichko et al., 2007*], when in the vast territories of Western Siberia, under conditions of permafrost, the unique periglacial landscapes were being formed having no recent analogues.

The authors thank the corresponding member of the Russian Academy of Sciences, Doctor of Biological Sciences A.O. Alekseev, Ph.D. T.V. Alekseeva and Ph.D. P.I. Kalinin (Institute of Physicochemical and Biological Problems in Soil Science, RAS, Pushchino) for conducting analytical determinations, Ph.D. F.E. Maksimov (St. Petersburg State University) and Ph.D. V.E. Tumskoy (Moscow State University) for valuable advice.

The work has been carried out according to the state task (project AAAA-A17-117051850064-0), with partial financial support from the Russian Federal Property Fund (project No. 20-05-00734A).

References

Alekseev, A.O., Kalinin, P.I., Alekseeva, T.V., 2019. Soil indicators of paleoenvironmental conditions in the south of the East European Plain in the Quaternary Time. Eurasian Soil Science, No. 52 (4), 349–358.

Alekseeva, T.V., Alekseev, A.O., Gubin, S.V., 2016. Paleosol complex in the uppermost Mikhailovian horizon (Viséan, Lower Carboniferous) in the southern flank of the Moscow syneclise. Paleontological Journal, No. 4, 5–20.

Alekseeva, V.A., 2003. Displacement and diagenetic transformation of quartz grains and their paleogeographic interpretation. Vestnik Moskovskogo Universiteta. Ser. 5. Geografiya (Bulletin of Moscow University, Section 5. Geography), No. 4, 40–46.

Alekseeva, V.A., 2005. Micromorphology of quartz grain surface as indicator of glacial sedimentation conditions: evidence from the Protva River basin. Lithology and Mineral Resources 40 (5), 420–428.

Arkhipov, S.A., 1971. Quaternary Period in Western Siberia. Nauka, Novosibirsk, 332 pp. (in Rissian).

Baulin, V.V., Chekhov, A.L., Sukhodolsky, S.E., 1981. Main stages of development of permafrost rocks of the European North-East and Western Siberia. In: History of Development of Permafrost Rocks of Eurasia. Nauka, Moscow, pp. 41–60 (in Russian).

Cox, R., Lowe, D.R., Cullers, R.L., 1995. The influence of sediment recycling and basement composition on evolution of mudrock chemistry in southwestern United States. Geochim. et Cosmochim. Acta 59, 2919–2940.

Derevyanko, A.P., Molodin, V.I., Zenin, V.N., et al., 2003. Upper Paleolithic location Shestakovo. Institut Arkheologii i Etnografii SO RAN, Novosibirsk, 168 pp. (in Russian).

Dynamics of landscape components and internal sea basins of Northern Eurasia over the past 130,000 years, 2002. Atlas-monograph "The development of landscapes and climate of Northern Eurasia. Late Pleistocene–Holocene – elements of forecast. Issue II. General Paleogeography". GEOS, Moscow, 232 pp. (in Russian).

Fedo, C.M., Nessbitt, H.W., Young, G.M., 1995. Unraveling the effects of potassium metasomatism in sedimentary rock and paleosols, with implications for paleoweathering conditions and provenance. Geology 23, 921–924.

Fedorovich, B.A., 1962. Permafrost formations in the steppe and desert regions of Eurasia. In: Questions of stratigraphy and paleogeography of the Quaternary period. Proceedings of the Commission on Quaternary period study. Izd-vo AN SSSR, Moscow, vol. XIX, pp. 70–100 (in Russian).

Fotiev, S.M., 2009. Cryogenic Metamorphism of Rocks and Underground Waters (conditions and results). Acad. Izd-vo "Geo", Novosibirsk, 279 pp. (in Russian).

Frolov, V.T., 1993. Litology, Vol. 2. Moskow University Press, Moscow, 432 pp. (in Russian).

Gallet, S., Jahn, B., Torii, M., 1996. Geochemical characterization of the Luochuan loess-paleosol sequence, China, and paleoclimatic implications. Chemical Geology 133, 67–88.

Gorbunova, T.A., Osintseva, N.V., Shmidt, I.V., Shtoible, Kh., 2016. New data on the geomorphology, stratigraphy and dating of the station Chernoozerie II. In: Eurasia in the Cenozoic. Stratigraphy, Paleoecology, Culture. Izd-vo IGU, Irkutsk, vol. 5, pp. 153–157 (in Russian).

Kalinin, P.I., Alekseev, A.O., 2013. Geochemical approach to the study of the origin of loess deposits in the South-East of the Russian Plain. Vestn. Voronezh. Gos. Un-ta. Ser. Geologiya (Bulletin of Voronezh State University. Section Geology), No. 2, 53–60.

Kalinin, P.I., Alekseev, A.O., Savko, A.D., 2009. Loesses, Paleosol sand Paleogeography of Quaternary Period of the South-East of the Russian Plain. Voronezhskiy Gos. Un-t, Voronezh, 139 pp. (in Russian).

Kaplyanskaya, F.A., Tarnogradsky, V.D., 1972. Pleistocene cryogenic phenomena and the history of permafrost in Western Siberia. In: Stratigraphy, Sedimentology and Geology of the Quaternary Period. Nauka, Moscow, pp. 47–57 (in Russian).

Khabakov, A.V., 1946. About the indexes of roundness of pebbles. Sovetskaya Geologiya (Soviet Geology), No. 10, 98–99.

Konishchev, V.N., 1999. Evolution of rock's temperature of the Russian Arctic zone in the Late Cenozoic. Kriosfera Zemli (Earth's Cryosphere), III (4), 39–47.

Konishchev, V.N., Lebedeva-Verba, M.P., Rogov, V.V., Stalina, E.E., 2005. Cryogenesis of Modern and Late Pleistocene Sediments of Altai and Europe Periglacial Areas. GEOS, Moscow, 133 pp. (in Russian).

Konishchev, V.N., Rogov, V.V., 1994. Methods of Cryolithological Research. Moscow University Press, Moscow, 131 pp. (in Russian).

Konishchev, V.N., Rogov, V.V., 2016. The evidence of cryogenic processes in loess. Kriosfera Zemli (Earth's Cryosphere), XX (4), 37–44.

Krinsley, D.H., Doornkamp, J.C., 2011. Atlas of Quartz Sand Surface Textures. Cambridge University Press, Cambridge, 102 pp.

Larin, S.I., Alekseeva, V.A., Alekseev, A.O., et al., 2018. Cryogenic structures and drying cracks in the southwest of the West Siberian plain. In: Proceeding of the Extended Meeting of the Scientific Council on Earth Cryology RAS "Actual problems of Geocryology" with the participation of Russian and foreign scientists, engineers and specialists (Moscow, May 15–16, 2018). KDU, Univ. Kniga, Moscow, vol. 1, pp. 276–281 (in Russian).

Larin, S.I., Alekseeva, V.A., Laukhin, S.A., et al., 2016. On the origin of relict ground veins in the upper neo-Pleistocene sediments in the southwest of the West Siberian plain. In: Proceeding of the Fifth Conference of Geocryologists (Moscow, June 14–17, 2016). Univ. Kniga, Moscow, vol. 2, pp. 188–195 (in Russian).

Larin, S.I., Larina, N.S., Laukhin, S.A., et al., 2015. New data on the variability of paleogeographic conditions of the Late neo-Pleistocene in Western Siberia (based on the study of the Lipovka reference section). In: Actual problems of Pleistocene paleogeography and stratigraphy: Proceedings of the all-Russia Conference "Markov readings–2015". Moscow State University, Moscow, pp. 100–102 (in Russian).

Laukhin, S.A., Larin, S.I., Guselnikov, V.L., 2012. The first findings of ancient permafrost traces in the Kurgan region. Vestnik TyumGU. Nauki o Zemle (Bulletin of TyumSU. Earth Sciences), No. 4, 104–112.

Lozano, R., Bernal, J.P., 2005. Characterization of a new set of eight geochemical reference materials for XRF major and trace element analysis. Revista Mexicana de Ciencia Geológicas 22 (3), 329–344.

Lukashev, V.K., 1970. Geochemistry of Quaternary Lithogenesis. Nauka i Tekhnika, Minsk, 528 pp. (in Russian).

Mahaney, W.C., 2002. Atlas of Sand Grain Surface Textures and Applications. Oxford University Press, New York, 237 pp.

Nesbitt, H.W., Young, G.M., 1982. Early Proterozoic climates and plate motions inferred from major element chemistry of lutites. Nature 299, 399–429.

Osintseva, N.V., 2017. The crest relief of the South of the West Siberian plain: morphology and age (on the example of Chernoozerskaya mane, Sargat region). Geospherniye Issledovaniya (Geosphere studies), No. 3, 26–32.

Perelman, A.I., 1989. Geochemistry. Vysshaya shkola, Moscow, 528 pp. (in Russian).

Petrin, V.T., 1986. Paleolithic Monuments of the West Siberian Plain. Nauka, Novosibirsk, 142 pp. (in Russian).

Reimer, P.J., Bard, E., Bayliss, et al., 2013. IntCal13 and Marine13 radiocarbon age calibration curves 0–50,000 years cal BP. Radiocarbon 55 (4), 1869–1887.

Retallac, G.J., 2001. Soils of the Past: An Introduction to Paleopedology. 2nd ed. Blacwell, Oxford, 600 pp.

Retallac, G.J., 2003. Soils and global change in the carbon cycle over geological time. Treatise on Geochemistry 5, 581–605.

Rogov, V.V., 2009. The Basics of Cryogenesis (educational and methodical manual). Acad. Izd-vo "Geo", Novosibirsk, 203 pp. (in Russian).

Romanovsky, N.N., 1977. Formation of Polygonal Structures. Nauka, Novosibirsk, 215 pp. (in Russian).

Schilman, B., Bar-Matthews, M., Almogi-Labin, A., Luz, B., 2001. Global climate instability reflected by Eastern Mediterranean marine records during the late Holocene. Palaeogeography, Palaeoclimatology, Palaeoecology 176, 157–176.

Sheldon, N.D., Tabor, N.J., 2009. Quantitative paleoenvironmental and paleoclimatic reconstruction using paleosols. Earth-Sci. Rev. 95, 1–52.

Syso, A.I., 2007. The Patterns of Chemical Elements Distribution in Soil-forming Rocks and Doils of Western Siberia. Izd-vo SO RAN, Novosibirsk, 277 pp. (in Russian).

Velichko, A.A. (Ed.), 2009. Paleoclimates and paleolandscapes of the extratropical area of the Northern hemisphere. Late Pleistocene–Holocene. Atlas-monograph. GEOS, Moscow, 120 pp. (in Russian).

Velichko, A.A., Timireva, S.N., Kremenetskiy, K.V., et al., 2007. West Siberian Plain in the image of the late-glacial desert. Izv. RAN. Ser. Geographicheskaya (Proceedings of Russian Academy of Sciences, Section of Geography), No. 4, 16–28.

Vlag, P.A., Kruiver, P.P., Dekkers, M.J., 2004. Evaluating climate change by multivariate statistical techniques on magnetic and chemical properties of marine sediments (Azores region). Palaeogeography, Palaeoclimatology, Palaeoecology 212, 23–44.

Volkov, I.A., Volkova, V.S., Zadkova, A.A., 1969. Cover loess-like deposits and paleogeography of South-West Western Siberia in Pliocene-Quaternary. Nauka, Novosibirsk, 332 pp. (in Russian).

Voronin, A.D., 1986. Basics of Soil Physics. Moscow University Press, Moscow, 244 pp. (in Russian).

Vos, K., Vandenberghe, N., Elsen, J., 2014. Surface textural analysis of quartz grains by scanning electron microscopy (SEM): From sample preparation to environmental interpretation. Earth-Science Reviews 128, 93–104.

Zeitlin, S.M., 1979. Geology of the Paleolithic Age of Northern Asia. Nauka, Moscow, 286 pp. (in Russian).

Zeitlin, S.M., 1985. Geology of the upper Paleolithic station Chernoozeje II. In: V.F. Gening, V.T. Petrin (Eds.). Late Paleolithic Era in the South of Western Siberia. Nauka, Novosibirsk, pp. 67–71 (in Russian).

Zubakov, V.A., 1970. Paleogeography and geochronology of Upper Pleistocene and Holocene of Western Siberia. Izv. AN SSSR. Ser. Geographiya (Bulletin of the USSR Academy of Sciences, Section Geography), No. 3, 36–45.

Zykin, V.S., Zykina, V.S., Orlova, L.A., 2001. Basic regularities of changes in the natural environment and climate in the Pleistocene and Holocene of Western Siberia. In: Global changes in the natural environment. Izd-vo SO RAN, Novosibirsk, pp. 208–228 (in Russian).

Received July 10, 2019
Revised version received November 1, 2019
Accepted March 11, 2020